Supplementary Materials and Methods

Lysate preparation and western blotting

Freshly excised mammary glands were snap frozen in liquid nitrogen and homogenized using a Pro-Scientific homogenizer in RIPA lysis buffer (50 mM Tris chloride pH 7.5, 100 mM NaF, 0.1% SDS, 1 mM EDTA, 1 mM PMSF, 10 µg/ml Aprotinin, 10 µg/ml Leupeptin, 1 mM Na3VO4, and 0.02% NP-40) (Sakamoto et al., 2007). Mammary organoid lysates were prepared in the same lysis buffer. Lysates were resolved on 8-10% SDS-PAGE and transferred to PVDF membranes, which were blocked with 2% BSA in Tris-buffered saline (TBS) and incubated overnight at 4°C with specific antibodies diluted in TBS-T (TBS, 0.1% Tween-20). Membranes were washed three times in TBS-T, incubated with HRP-conjugated species-specific secondary antibodies (Zymed Laboratories) and signals were detected with Pierce ECL substrate (Thermo Scientific).

Real-time quantitative PCR (qPCR)

FACS-sorted cells were directly collected in Trizol reagent (Ambion, Life Technology) for RNA extraction. cDNA was obtained by reverse transcription using the Invitrogen SuperScript III system (18080-051), and real-time qPCR was done using the SYBR Green labeling method (Applied Biosystems; 4309155) on a Bio-Rad CFX-96 Thermo Cycler. Primer sequences (Sigma-Aldrich) are listed in Table S3. Relative gene expression was calculated according to the ΔCt method, and normalized to Gapdh reference gene expression. A representative of three independent cell-sorting experiments is presented.

References

Sakamoto, K., Creamer, B. A., Triplett, A. A. and Wagner, K. U. (2007). The Janus Kinase 2 is Required for Expression and Nuclear Accumulation of Cyclin D1 in Proliferating Mammary Epithelial Cells. *Mol. Endocrinol.* **21**, 1877-1892.

Naramura, M., Nandwani, N., Gu, H., Band, V. and Band, H. (2010). Rapidly Fatal Myeloproliferative Disorders in Mice with Deletion of Casitas B-Cell Lymphoma (Cbl) and Cbl-B in Hematopoietic Stem Cells. *Proc. Natl. Acad. Sci. U. S. A.* **107**, 16274-16279.

Wagner, K. U., McAllister, K., Ward, T., Davis, B., Wiseman, R. and Hennighausen, L. (2001). Spatial and Temporal Expression of the Cre Gene Under the Control of the MMTV-LTR in Different Lines of Transgenic Mice. *Transgenic Res.* **10**, 545-553.

Supplementary Figures:

A.

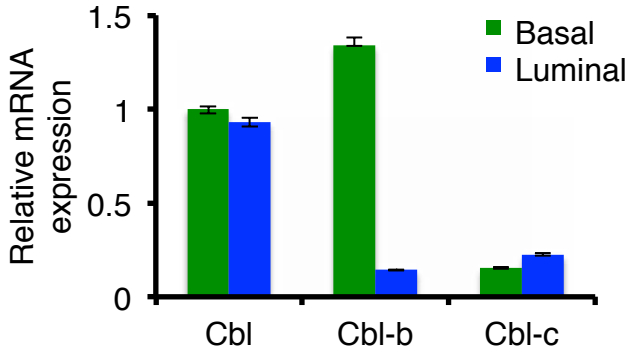

B.

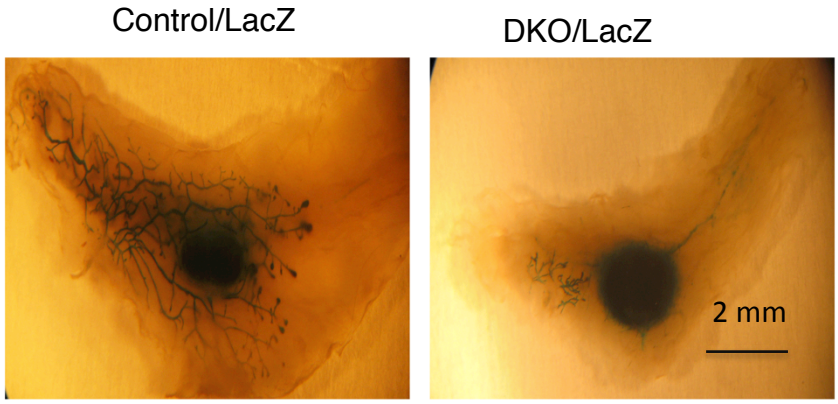

C.

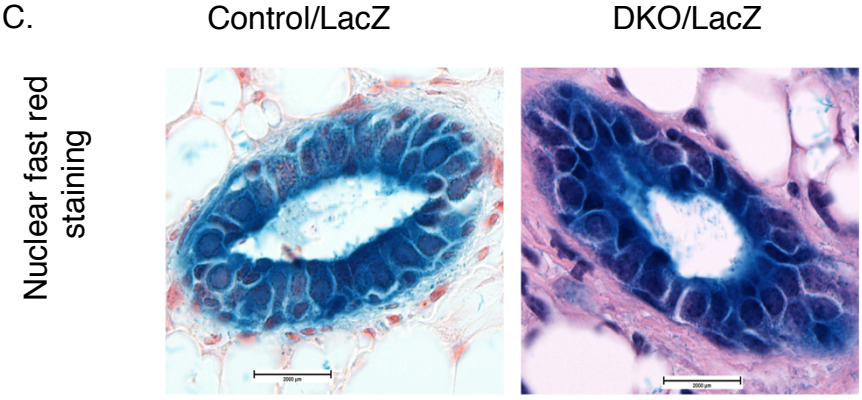

D.

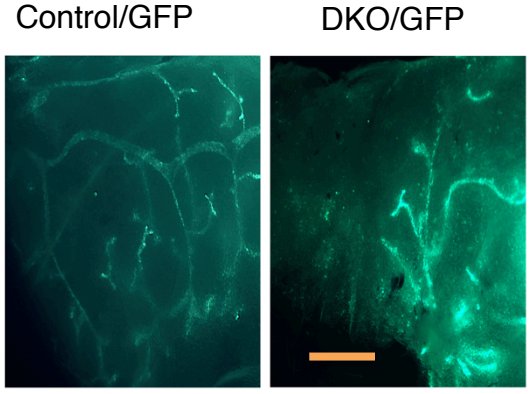

Figure S1. Quantitative PCR analysis of the expression of CBL family members in mammary epithelial cells and verification of MMTV-Cre-mediated recombination in *Cbl/Cbl-b* DKO mammary glands using reporter genes. (A) Real time quantitative PCR (qPCR) using primer sets specific for CBL, CBL-B or CBL-C was performed on mRNA isolated from FACS-isolated basal ($CD29^{hi}EpCAM^{low}$) and luminal ($CD29^{low}EpCAM^{hi}$) compartments of normal mouse mammary gland. Values are expressed relative to GAPDH, used as an internal reference. Data shown are mean +/- SEM, n=3. (B) Mammary glands of 6-week old *Cbl/Cbl-b* DKO and control mice carrying a LacZ reporter allele were stained with x-gal to visualize the distribution of β-galactosidase activity, which is seen in the epithelium and not the stroma. Staining of lymph node is due to concurrent deletion in the hematopoietic system, as previously described (Naramura et al., 2010;Wagner et al., 2001). (C) Nuclear fast red (counterstains nuclei as pink) and X-gal staining was performed to reveal MMTV-Cre-mediated targeted gene deletion in both luminal and basal compartments. (D) Fluorescent microscopy analysis to visualize GFP expression in the mammary ducts of DKO and control mice carrying a GFP reporter allele. Scale bar represents 500 μM.

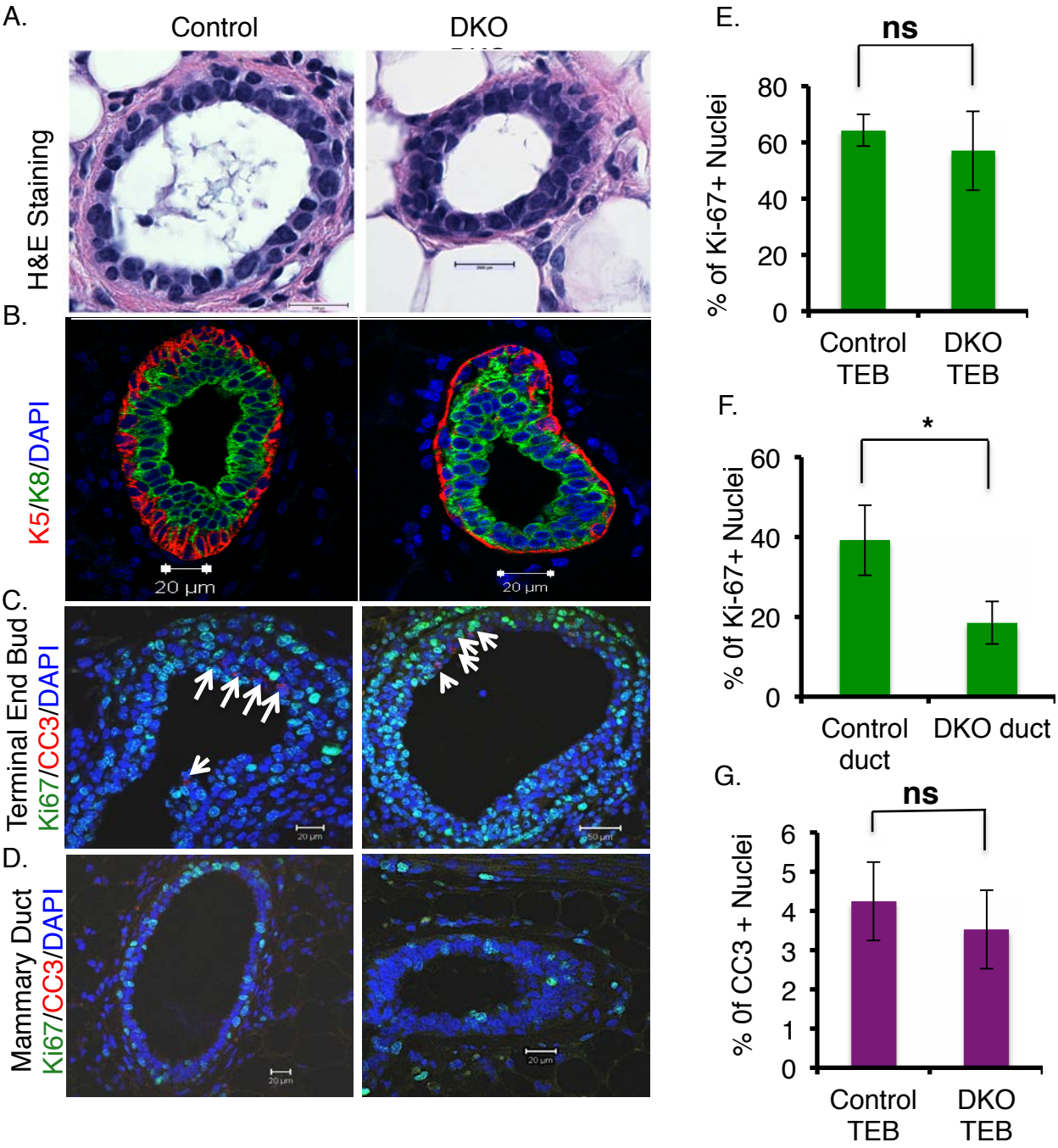

Figure S2. Histological and immuno-histological analyses of mammary gland to assess the impact of MMTV-Cre-mediated *Cbl/Cbl-b* DKO. (A) Hematoxylin and eosin (H&E) staining of formaldehyde-fixed and paraffin-embedded tissue sections of 6-week old *Cbl/Cbl-b* DKO and control mammary glands to show the lack of any obvious architectural defects in DKO mammary glands. (B) Immunofluorescence (IF) staining of *Cbl/Cbl-b* DKO and control mammary gland sections for basal (K5, red) and luminal (K8, green) cytokeratins. No differences in the luminal/basal organization are seen between DKO and control mammary glands. (C, D) Mammary gland sections from 6-week old control and DKO mice were stained with anti-Ki67 (green) and anti-cleaved caspase 3 (CC3, red) antibodies to visualize the proliferating and apoptotic cells within the terminal end buds and mammary ducts. Quantification was performed by scanning at least 15 high-power fields for proliferating (Ki67+) (E, F) and apoptotic (CC3+) (G) cells. Terminal end buds in control and DKO mammary glands show comparable levels of proliferation (E) and apoptosis (G). Mammary ducts in DKO mammary glands show a lower percentage of proliferating cells (F). Apoptotic events in mammary ducts were below the detection limit. Data shown are mean ± SEM, n=4 (independent sets). *, $p \leq 0.05$; ns, $p \geq 0.05$ (Student's t test).

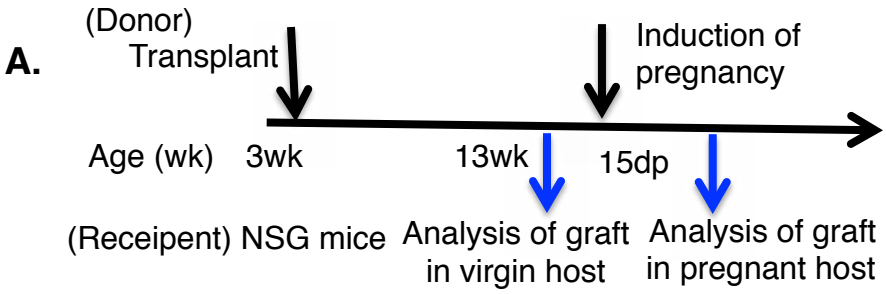

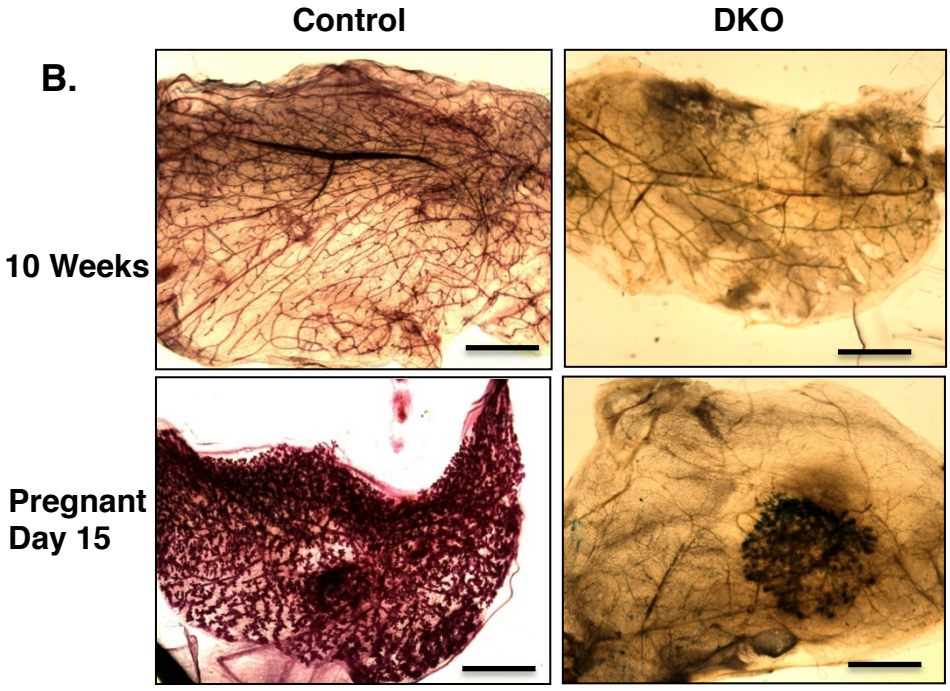

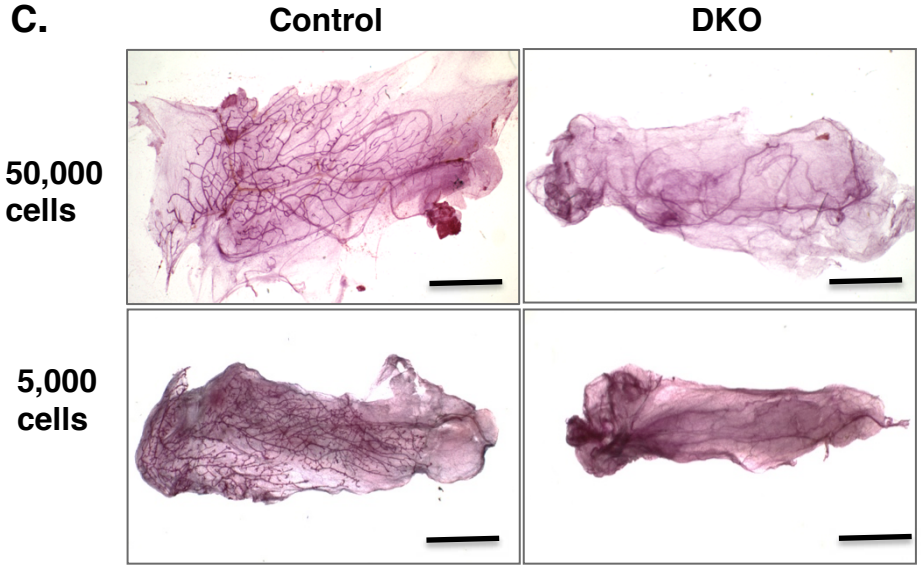

D.

Subsets	Genotype	# Cells	Take rate
Lin⁻ Unsorted	Control	50,000	5/5
	DKO	50,000	0/5
Lin⁻ EpCAM⁺	Control	5,000	4/7
	DKO	5,000	0/7

Figure S3. Reduced growth and branching of *Cbl/Cbl-b* DKO mammary glands upon transplantation, and defective mammary gland regenerating ability of isolated DKO mammary epithelial cells. (**A**) Schematic showing the time-line of tissue transplants and their analysis**.** (**B**) Mammary tissue fragments from MMTV-Cre based *Cbl/Cbl-b* DKO and control mice were transplanted into cleared mammary fat pads of 3-week old NOD/SCID/Gamma chain-deficient (NSG) mice and analyzed after 10 weeks**.** Each host received DKO and control transplants on the opposite sides. Whole-mount Carmine staining was carried out to visualize the growth and branching of glands formed from the transplanted mammary fragments. Less ductal elongation and branching is seen in DKO compared to control transplant. In transplant recipients analyzed at day 15 of pregnancy), transplanted DKO mammary fragments show a severe defect in ductal elongation compared to control although alveologenesis appears intact. Scale bar is 1 mm. (**C**) Lineage-negative mammary epithelial cells or $EpCAM^{+}$ epithelial cells from DKO or control mice were injected into cleared mammary fat pads on opposite sides of 3-week old NSG mice. Whole mounts of transplanted mammary fat pads were analyzed after 8 weeks to assess the ductal outgrowth. (**D**) Relative success of generating mammary outgrowths from transplanted mammary epithelial cells from control vs. DKO mice. Numbers in the last column indicate those positive for outgrowths vs. the total number transplanted (Take rate).

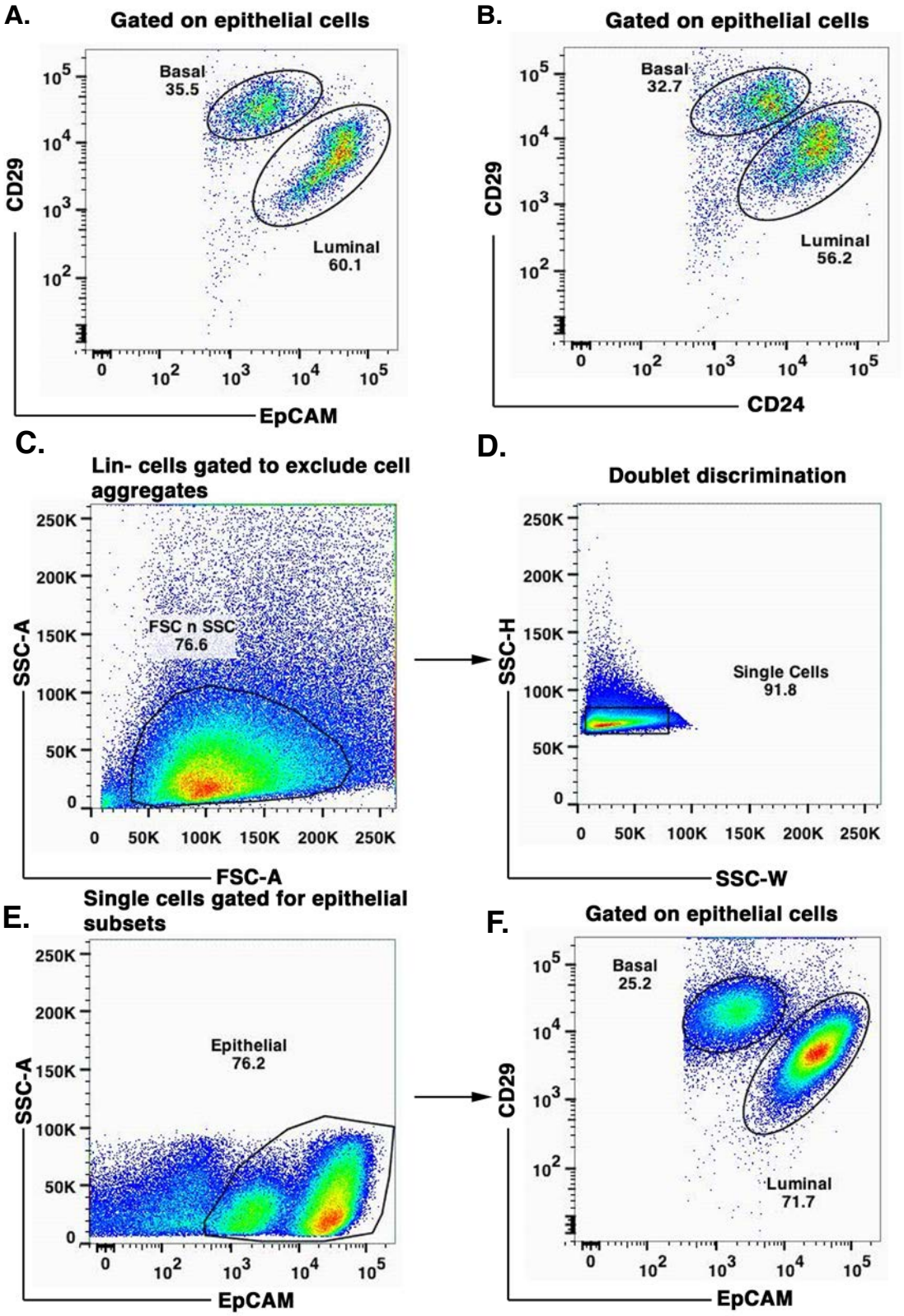

Figure S4. Typical plots of FACS-based separation of basal and luminal mammary epithelial cell populations using CD24 and EpCAM surface markers and the gating scheme used. Live Lin-negative (Lin-) cells were stained with fluorophore-labeled antibodies against mammary stem cell surface markers CD29, EpCAM or CD24. FACS plots showing the distribution of mammary epithelial cell populations from the same donor mouse when double-stained for CD24 and CD29 (A) or CD29 and EpCAM (B) marker combinations display comparable luminal and basal epithelial cell profiles, but better separation of the two fractions using CD29 and EpCAM combination. The flow cytometry gates based on forward (FSC) and side scatter (SSC) were used for exclusion of cell aggregates and dead cells (C), and to discriminate cell doublets from dual staining of single cells. (D). Gates used to demarcate the epithelial from stromal cells in double-staining analyses (E) and further separation of basal and luminal populations (F) are shown.

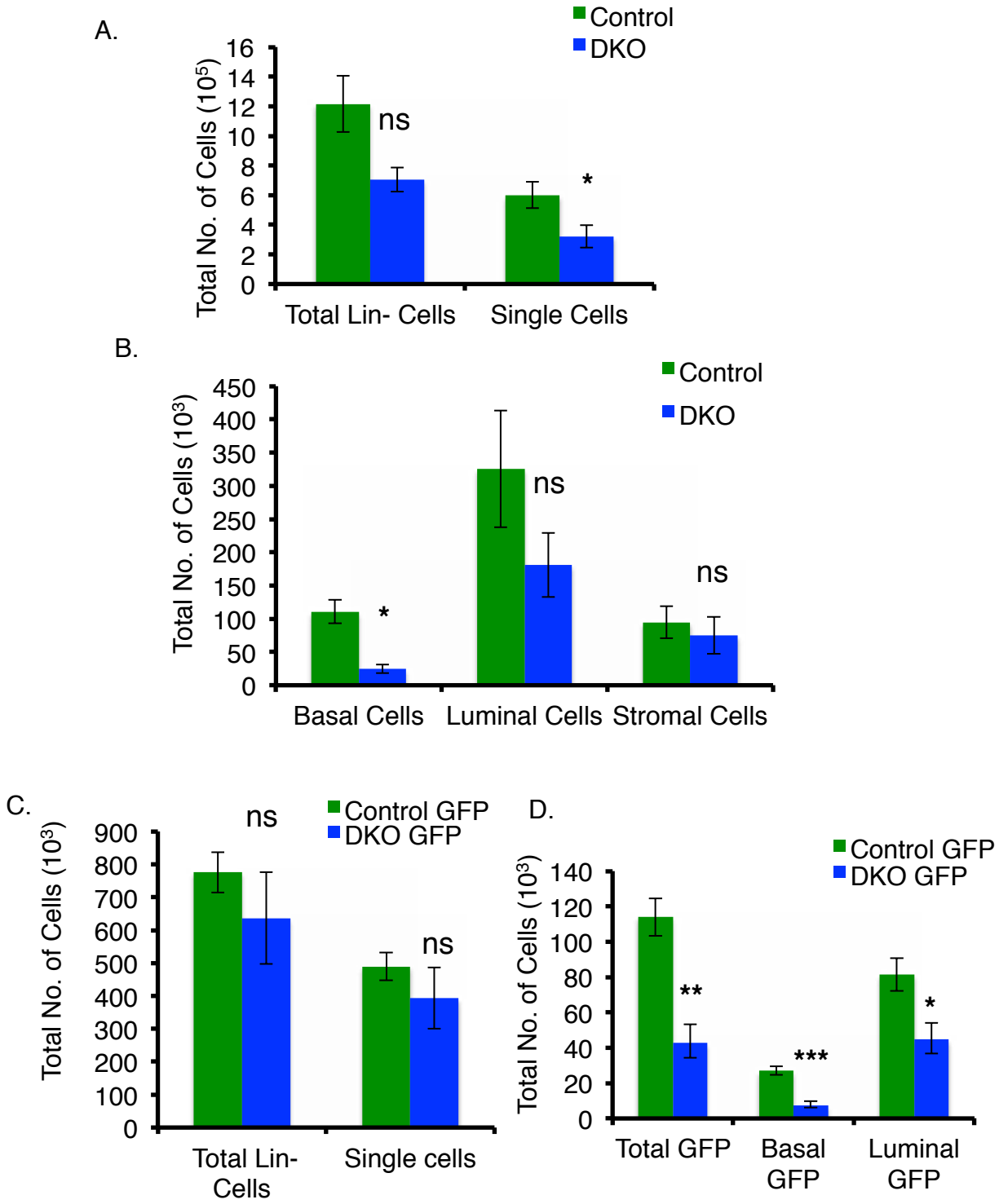

Figure S5. Reduction in the number of total mammary epithelial cells in MMTV-Cre-based *Cbl/Cbl-b* DKO mice as assessed by FACS analysis. (A-B) Lineage-negative mammary epithelial populations isolated from mammary glands of control or *Cbl/Cbl-b* DKO mice were gated for single cells by excluding doublets and dying cells as in Fig. S3 (A), and further gated to quantify the basal, luminal, and stromal populations (B). These analyses (n=6) show reduced yield of total Lin- single cells (A) and a selective reduction in the basal mammary epithelial cell pool in *Cbl/Cbl-b* DKO vs. the control mice. (C-D) Control or *Cbl/Cbl-b* DKO mice carrying a GFP reporter that is expressed after MMTV-Cre-mediated recombination were analyzed as in A-B. While differences in the numbers of total Lin- cells and single cells were not significant (C), the reduction in the numbers of GFP+ total single cells, basal cells and luminal cells was significant.

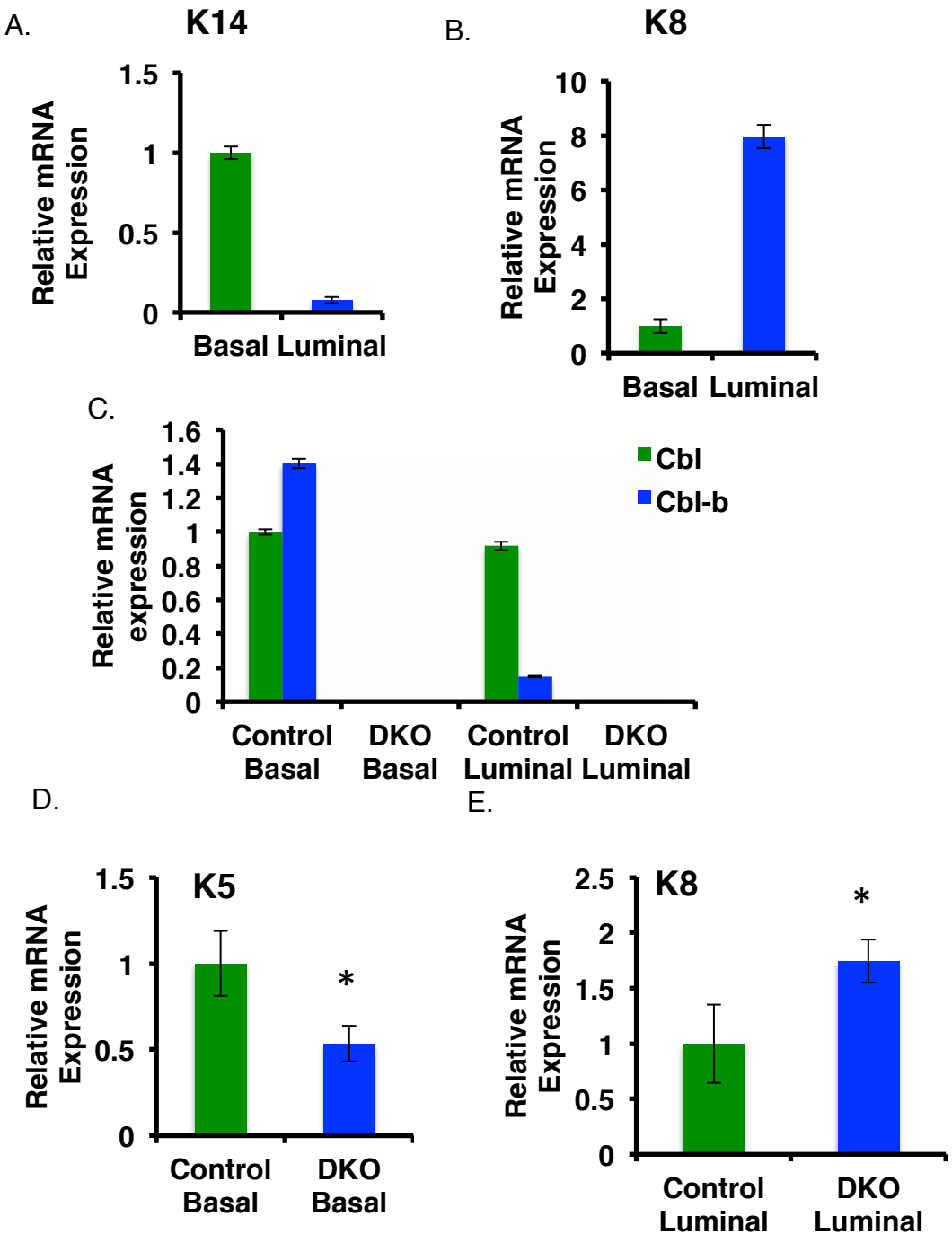

Figure S6. Demonstration of the lack of CBL and CBL-B expression in isolated mammary epithelial subsets. (A) The GFP+ cells within the basal and luminal subpopulations of isolated single mammary epithelial cell (as in Fig. S4C-D) were FACS-sorted based on CD29/EpCAM staining, and used to isolate RNA. The purity of sorted cells was analyzed by qPCR using primer sets specific to basal cytokeratin *K14* (A) or luminal cytokeratin *K8* (B), respectively. The basal population is enriched for cytokeratin *K14* while luminal cells are enriched for cytokeratin *K8*. (C) qPCR analysis was performed to quantify *Cbl* and *Cbl-b* mRNA expression relative to *GAPDH* as an internal reference control. Note the higher *Cbl-b* expression in the control basal compared to luminal population. Expression of both *Cbl* and *Cbl-b* is absent in DKO cell subsets. Concurrent qPCR analysis revealed reduced basal cytokeratin *K5* (D) and increased luminal cytokeratin *K8* (E) expression in DKO compared to control mammary cell subsets. Data shown are mean +/- SEM (n=3). ns, $p \geq 0.05$; *, $p \leq 0.05$, **, $p \leq 0.01$, ***, $p \leq 0.001$ by Student's t test.

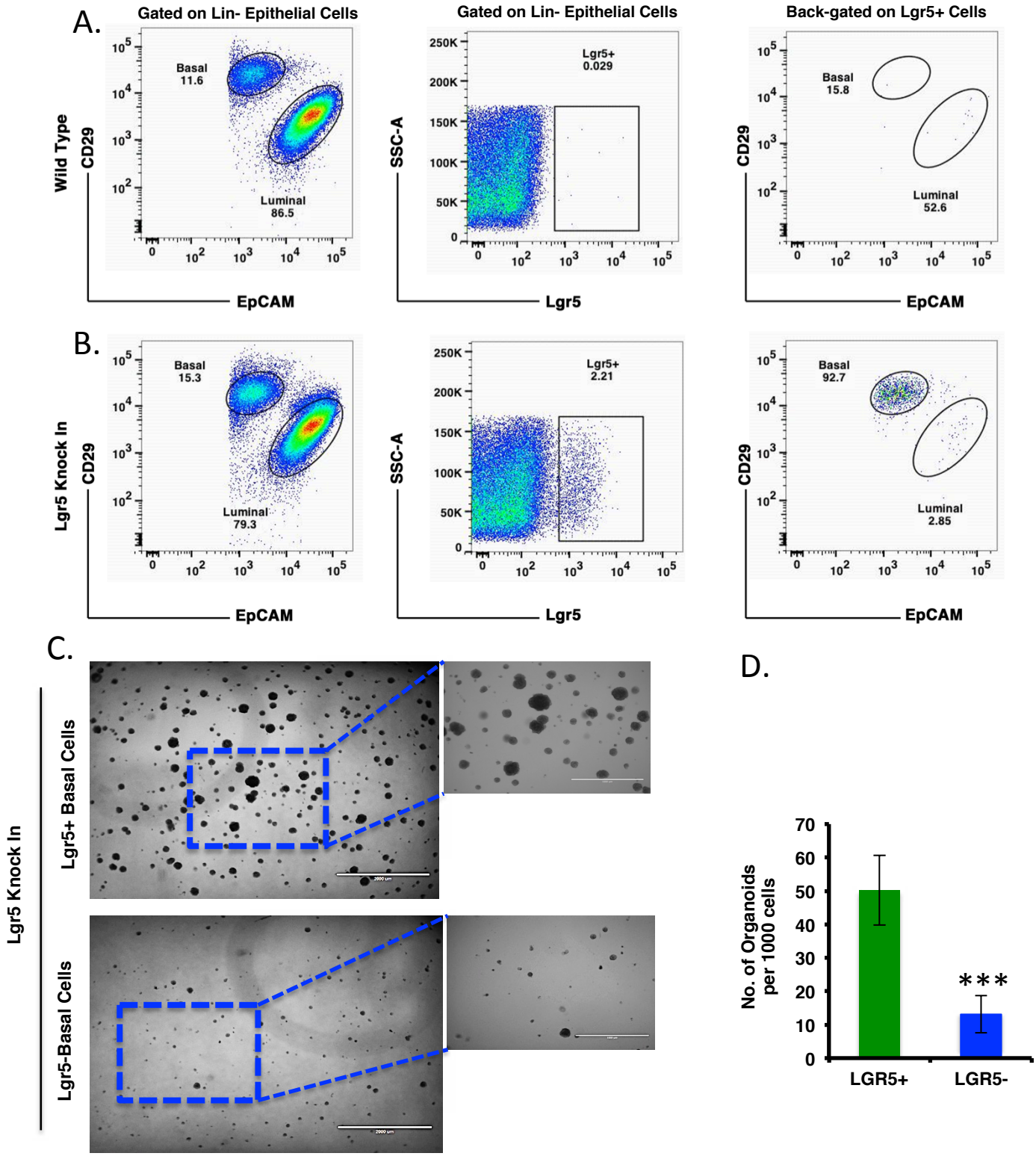

Figure S7. Compartmentalization of Lgr5+ mammary epithelial cells within the basal population, and validation of their self-renewal using the in vitro organoid-forming assay. Lineage-negative cells isolated from 5-week old WT (A) or Lgr5-GFP-IRES-CRE-ERT2 knock-in (Lgr5-GFP-Cre) (B) mice were analyzed by FACS for CD29, EpCAM and GFP. GFP+ cells (representing Lgr5+ cells) comprised 1-3% of epithelial cells; such cells were absent in WT MECs (upper panel), establishing the specificity of FACS-based analysis. Back-gating onto CD29/EpCAM-based subsets shows the majority of GFP+ cells to be within the basal cell compartment. The rare WT control cells seen within the GFP gate (<0.1%) did not specifically compartmentalize within the basal population. (C) The Lgr5+ (GFP+) and Lgr5- (GFP-) basal cells were isolated from Lgr5-GFP-IRES-CRE-ERT2 knock-in (Lgr5-GFP-Cre) mice, and analyzed in the organoid-forming assay. (D). Quantification of the organoid-forming assay data, shown as mean +/- SEM (n=3). ns, $p \geq 0.05$; *, $p \leq 0.05$; **, $p \leq 0.01$; ***, $p \leq 0.001$, by Student's t test. Majority of organoid-forming ability resides in the Lgr5+ basal cell fraction.

A.

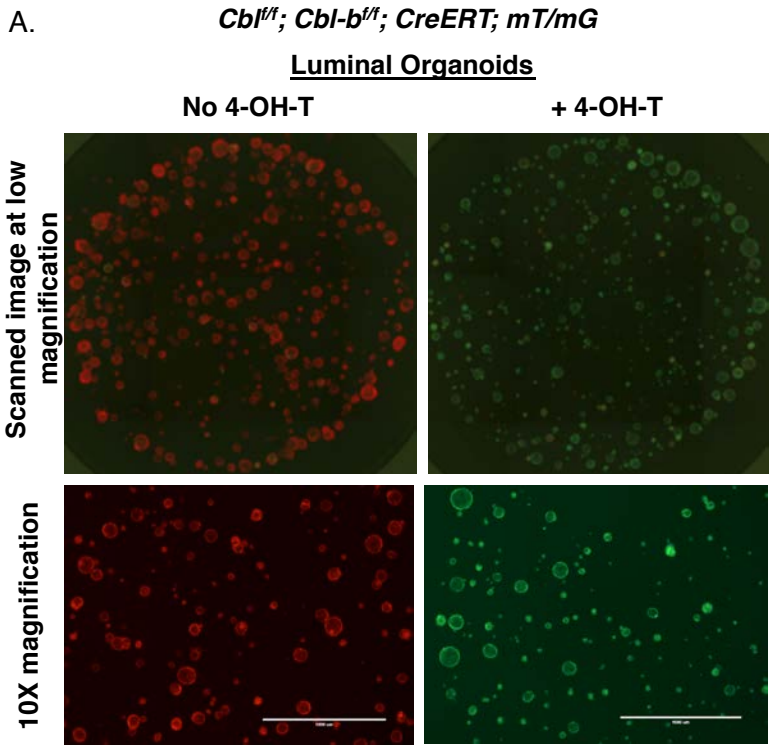

B.

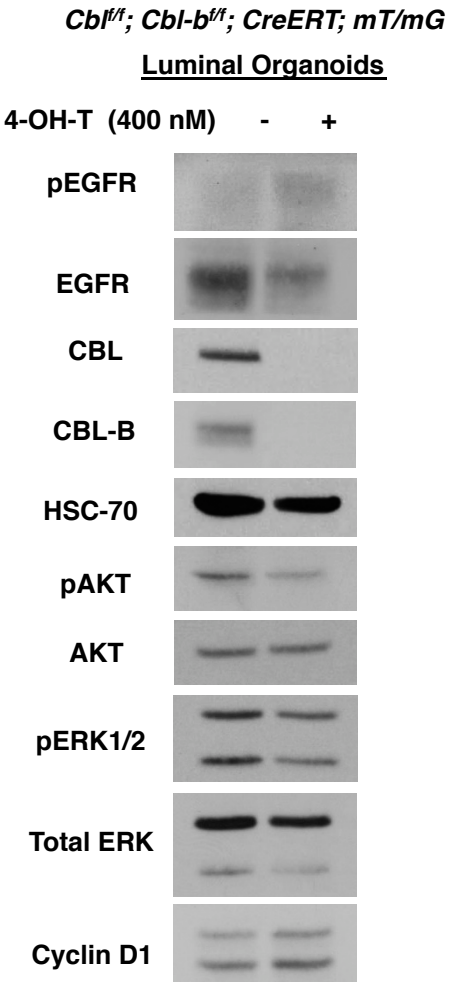

C.

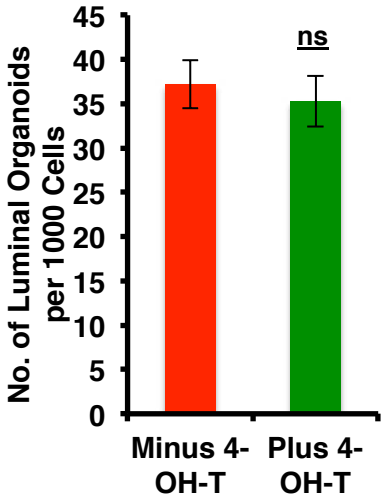

Figure S8. Luminal organoid-forming efficiency is unaltered upon tamoxifen-induced, CreERT-mediated, in vitro deletion in a model of *Cbl/Cbl-b* double-floxed model. (**A**) Luminal mammary epithelial cells isolated from 8 week-old *Cbl$^{f/f}$; Cbl-b$^{f/f}$; CreERT; mT/mG* (conditional DKO) were established in organoid cultures and treated with or without 4-OH-T to induce *Cbl/Cbl-b* deletion, as in earlier figures; the gene deletion is tracked using the dual fluorescent reporter). The non-induced or 4-OH-T-induced primary organoids formed by isolated luminal cells from *Cbl$^{f/f}$; Cbl-b$^{f/f}$; CreERT; mT/mG* (conditional DKO) to assess the self-renewal ability. Loss of red (RFP) and gain of green (GFP) fluorescence indicates successful CreERT activation and *Cbl/Cbl-b* deletion, which was confirmed by blotting, (B). (C) Quantitation of organoid numbers from (A). Data are shown as mean +/- SEM**.** n=3; ns, p≥0.05, *, p≤ 0.05, **, p≤0.01, ***, p≤0.001 by *Student's t* test.

Table S1. Nomenclature of mouse strains and their genotypes as used in this study.

Designation	**Genotype**
Control	$Cbl^{f/+}$; Cbl-$b^{+/-}$; MMTV-Cre(0/0) or $Cbl^{f/f}$; Cbl-$b^{+/-}$; MMTV-Cre(0/0)
Cre Control	$Cbl^{f/+}$; Cbl-$b^{+/-}$; MMTV-Cre(Tg/0)
Cbl KO	$Cbl^{-/-}$
Cbl-b KO	$Cbl^{f/f}$; Cbl-$b^{-/-}$; MMTV-Cre(0/0)
DKO/LacZ	$Cbl^{f/f}$; Cbl-$b^{-/-}$; MMTV-Cre(Tg/0); R26R
DKO/GFP	$Cbl^{f/f}$; Cbl-$b^{-/-}$; MMTV-Cre(Tg/0); CAG-GFP
MaSC- DKO	$Cbl^{f/f}$; $Cbl^{-/-}$; Lgr5-eGFP-IRES-CRE-ERT; R26R
MaSC-Control	$Cbl^{f/+}$; $Cbl^{+/-}$; Lgr5-eGFP-IRES-CRE-ERT; R26R or Lgr5-eGFP-IRES-CRE-ERT
Conditional DKO	$Cbl^{f/f}$; $Cbl^{f/f}$; CreERT; mT/mG

Table S2. List of primers used for PCR-based genotyping of various alleles.

Gene Allele	**Forward 5'-3'**	**Reverse 5'-3'**
Cbl WT	AAGTTCCAAGCCTAGCCAGATAT GTGTGTG	TCCCCTCCCCTTCCCATGTTTT TAATAGACTC
Cbl del	TGGCTGGACGTAAACTCCTCTTCA GACCAATAAC	TCCCCTCCCCTTCCCATGTTTT TAATAGACTC
Cbl floxed	GTGGTGGCTTGCAATTATAATCCT ACCACTTAGG	GTTTGAGATGTCTGGCTGTGTACAC GCG
Cbl-b del	CCCAGCAAAAGTAGCCAATG	CTTGCAAAAAGGACTAAGATTC
Cbl-b floxed	GGCAGAACCACTGAGACACATTT A	GGCTGCCAAACTGCTACCCAGGAG
MMTV-Cre	GCGGTCTGGCAGTAAAAACTATC	GTGAAACAGCATTGCTGTCACTT
Lgr5-eGFP-IRES-CRE-ERT (WT)	CTGCTCTCTGCTCCCAGTCT	ATACCCCATCCCTTT TGAGC
Lgr5-eGFP-IRES-CRE-ERT (Mutant)	CTGCTCTCTGCTCCCAGTCT	GAACTTCAGGGTCAGCTTGC
R26R-LacZ	AATCCATCTTGTTCAATGGCCGAT C	CCGGATTGATGGTAGTGGTC
CAG-GFP	GCACTT GCTCTCCCAAAGTC	GTTATGTAACGCGGA ACT CC
Rosa 26 –mT/ mGFP	CTCTGCTGCCTCCTGGCTTCT	TCAATGGGCGGGGGTCGTT

Table S3. List of real time PCR primers used to detect mRNA levels of the indicated genes.

Target	**Forward 5'-3'**	**Reverse 5'-3'**
Cbl	AGCTGATGCTGCCGAATTT	TTGCAGGTCAGATCAATAGTGG
Cbl-b	GGAGCTTTTTGCACGGACTA	TGCATCCTGAATAGCATCAA
Cbl-c	GCCACCTGCCTGCCTTTGAC	GCTACTTGGAGAGGTGGCAAAG
K14	TGAGAGCCTCAAGGAGGAGC	TCTCCACATTGACGTCTCCAC
K5	GAGATCGCCACCTACAGGAA	TCCTCCGTAGCCAGAAGAGA
K8	AGATCACCACCTACCGCAAG	TGAAGCCAGGGCTAGTGAGT
GAPDH	CCTGGAGAAACCTGCCAAGTATG	AGAGTGGGAGTTGCTGTTGAAGT